# Polar Transmitter Pre-Distortion Technique Validated with 2.5G Mobile Communication Signals

P. M. Cabral†, L. Cabria¥, J. A. Garcia¥, J. C. Pedro†

† Instituto de Telecomunicações – Universidade de Aveiro, Campus Universitário de Santiago, 3810-193 Aveiro, Portugal
Phone: +351 234377900, Fax: +351 234377901, e-mail: pcabral@ua.pt and jcpedro@ua.pt

¥ Dept. Ing. de Comunicaciones, Universidad de Cantabria, Avda. Los Castros s/n, 39005 Santander, Spain
Phone: +34 942200887, Fax: +34 942201488, email: cabrial@unican.es and joseangel.garcia@unican.es

***Abstract* — This paper presents a polar transmitter pre-distortion technique validated with 2.5G mobile communication signals. The methodology used, [1], complements the drain bias modulation with a proper input drive level variation. This technique is believed to improve the linearity, while maintaining the efficiency of such transmitters, and it was validated in a real laboratory test setup.**

## I. INTRODUCTION

Nowadays, wireless communication systems use complex modulation formats where amplitude and phase signal components are combined to code the original source symbols. The performance of these state-of-the-art systems is dominated by the stringent compromise between spectral and power supply efficiencies, [2]. In the traditional transmitter architectures, the RF power amplifier (PA) has to process an amplitude and phase modulated carrier. So, this Cartesian architecture, suffers from an important drawback in power supply efficiency because high fidelity of the amplitude modulation format requires a highly linear but inefficient class A or AB PA.

This opened the door to the dawn of a new transmitter (Tx) paradigm, represented by the polar architecture. In a conventional polar Tx, [based on the envelope elimination and restoration (EER) or Khan amplifier [3]], shown in Fig. 1, the envelope is first eliminated by a limiter, to guarantee that the PA is driven by a constant envelope phase-modulated RF carrier, while its output is amplitude modulated via the drain voltage signal, $v_{DD}(t)$, according to the input envelope amplitude evolution. Since the PA can always be kept in saturation, it can be operated in a highly efficient class-E or class-F switched-mode (SM). Therefore, unbeatable levels of linearity and efficiency are expected from these Txs.

This EER technique led to the polar Tx, in which the amplitude and phase signals are independently treated until the last stage, the RF PA, Fig. 2. Thus, for efficiency reasons, similar to the ones presented for the EER architecture, this must be a SM device, operating in a highly efficient class-E or F mode whose excitation is a constant envelope modulated carrier, while the amplitude is dynamically restored through its supply voltage.

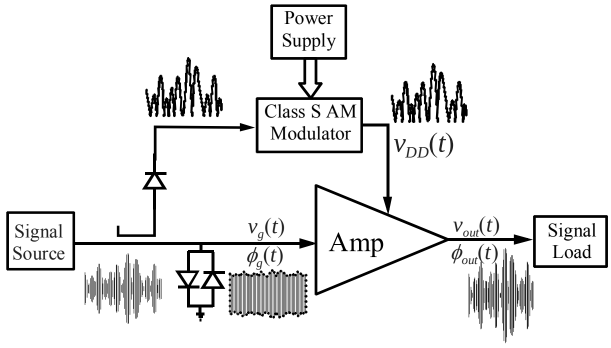


Fig. 1. EER Architecture.

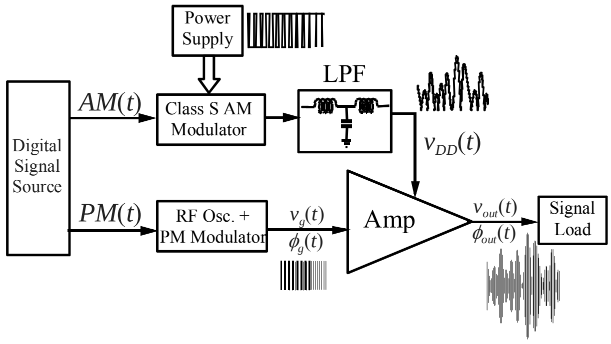


Fig. 2. Polar Transmitter Architecture.

In theory, such a Tx architecture would be 100% efficient and ideally linear. However, there are a series of system, circuit and device level reasons that justify why this cannot be met in practice [4]. In what the linearity is concerned, we can see that the SM RF PA, will present a nonlinear $v_{DD}$-to-$v_{out}$ characteristic.

Fig. 3 presents that characteristic for an HEMT based Class-E PA where is possible to see that, for vanishingly small $v_{DD}$ values, there will be a non-zero $v_{out}$. This phenomenon is due to the carrier feed-through (usually attributed to the RF carrier leakage via the input-output capacitance). For higher $v_{DD}$ values the $v_{DD}$-to-$v_{out}$ characteristic presents a certain degree of nonlinearity, typically determined by the transition between the switched and the current mode operation regimes, resulting in a slightly compressed AM/AM plot.

The first and fourth authors would like to thank to Portuguese Science Foundation, F.C.T., and Instituto de Telecomunicações for the financial support provided under Projects: PTDC/EEA-TEL/65988/2006 Digital_PAs and SWIPA Ref. Nr.: P423, respectively. The second and third authors would also like to thank the financial support given by MEC and CICE-JA through projects TEC2005-07985-C03-01/TCM and P07-TIC-2649, respectively.

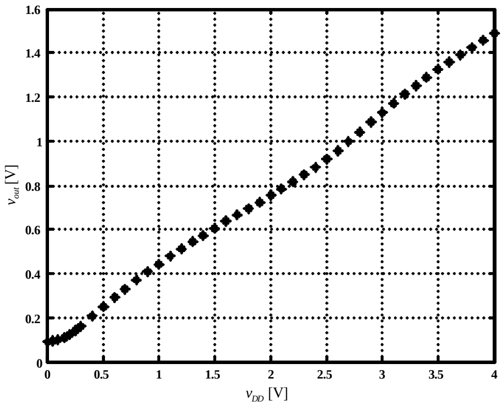


Fig. 3. $v_{DD}(t)$-to-$v_{out}(t)$ characteristic of a Class-E RF PA.

After having identified the linearity impairments, we can now concentrate on the efficiency. In this case, the issue is related to the undesirable instantaneous negative power added efficiency (PAE) that results when the amplitude envelope vanishes or is very small, which leads to a poor average PAE.

The idea is to use some kind of linearization technique capable of solving the above mentioned problems.

## II. LINEARIZATION PROCEDURE

Using the method presented in [1], that combines power supply modulation with a not-always-constant envelope driving signal, the $v_{in}(t)$ range is now divided in two distinct regions of operation.

For its highest values, and in order to maximize the time in which the PA is operated in SM, optimizing PAE, a constant $v_g(t)$ drive in applied to the RF PA input (EER operation) and a pre-distorted $v_{DD}[v_{in}(t)]$ modulation is employed.

For vanishingly small $v_{DD}$ values, this EER operation is complemented with envelope tracking (ET), selecting a proper $v_g[v_{in}(t)]$ variation to overcome the carrier-feed-through nonlinearity and instantaneous negative PAE. Finally, the characteristics are also accompanied by amplitude and phase linearization functions to compensate for any residual AM/AM and AM/PM nonlinearities. The design procedure can be summarized as follows:

The first step must be the characterization of the SM PA: $vout(v_{DD},v_g)$ and $\phi_{out}(v_{DD},v_g)$ curves leading to the selection of the maximum allowed excitation level that guarantees an EER operation, $v_{g\_M}$. The high end of this $v_{out}(v_{DD},v_{g\_M})$ characteristic will have to be linearized, defining the $v_{DD}(v_{in})$ voltage supply pre-distorter function. After that, the crossed $v_{out}(v_{DD},v_g)$ characteristics, in the low end of the $v_{out}(v_{DD})$ straight line, will be identified and the $v_g(v_{DD})$, and thus $v_g(v_{in})$, amplitude pre-distortion function determined. Finally, the $\phi_g(v_{in})$ phase pre-distortion function from the $\phi_{out}(v_{DD},v_g)$ plots will be determined, using the $v_g(v_{DD})$ and $v_g(v_{in})$ functions.

Fig. 4 presents the linearization technique schematic representation.

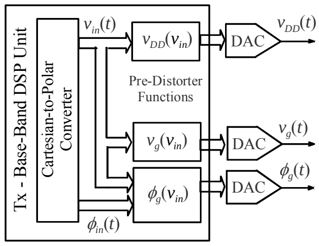


Fig. 4. Linearization technique schematic representation.

## III. EXPERIMENTAL SETUP

In order to validate the proposed pre-distortion method, we assembled a complete polar transmitter in the RF laboratory. Fig. 5 presents a schematic of the implemented test setup.

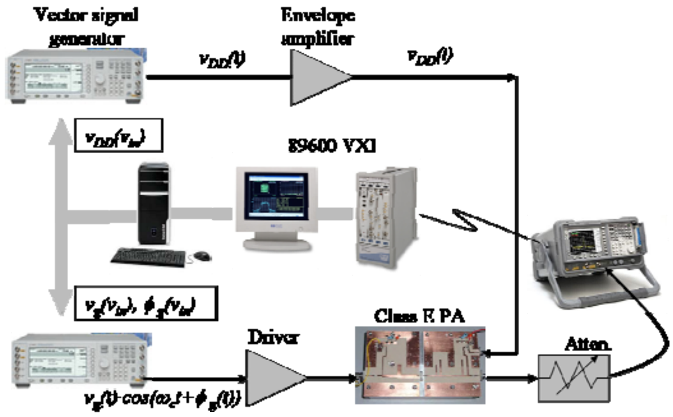


Fig. 5. Implemented test setup.

In this bench, two Agilent E4438C vector signal generators (VSG) are used to obtain the desired estimated $v_{DD}(t)$ (in one of them), and $v_g(t)$ and $\phi_g(t)$ signals (in the other). The output signals, either in frequency or in time domain, were obtained using Agilent's 89600 vector signal analyzer (VSA).

In what PA SM classes of operation are concerned, Class-E configuration, invented in 1975 by Sokal [5], has become the most popular and effective one. In terms of transistor technology, Gallium Nitride (GaN) HEMTs have already conquered their space because of their outstanding characteristics (high breakdown voltage, high power capabilities, high $f_t$, low input capacitance, manageable output capacitance and low ON-state resistance, $R_{ON}$) converting them into ideal solutions to implement SM PAs.

Our Class-E amplifier was designed following the transmission line topology proposed in [6]. The chosen transistor was a 15W GaN HEMT, from Cree, (model CGH35015F) and, as it can be seen in Fig. 6, which presents a photograph of the implemented PA, a drain biasing path was prepared to insert the low frequency envelope signal.

A PAE of 71% for an output power of 15 W was obtained when the device was biased at $V_{GS}$=-2.8V and $V_{DS}$=28V.

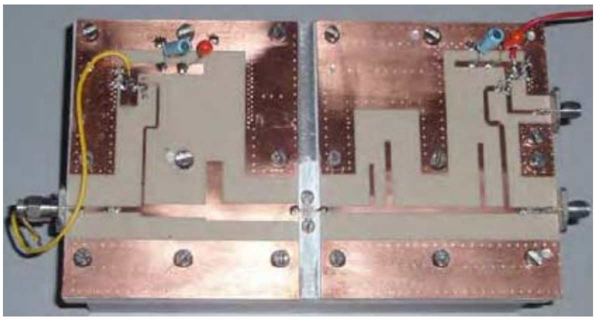

Fig. 6. Photograph of the implemented class E PA based on Cree CGH35015F GaN HEMT.

Fig. 7 a) and b) present the $v_{out}(v_{DD},v_g)$ and $\phi_{out}(v_{DD},v_g)$ characteristics of this particular RF SM PA. According to what was described in [1] and to the linearization procedure description presented in Section II of this paper, the identification of these $v_{out}(v_{DD},v_g)$ and $\phi_{out}(v_{DD},v_g)$ characteristics constitute the first step of the linearization procedure.

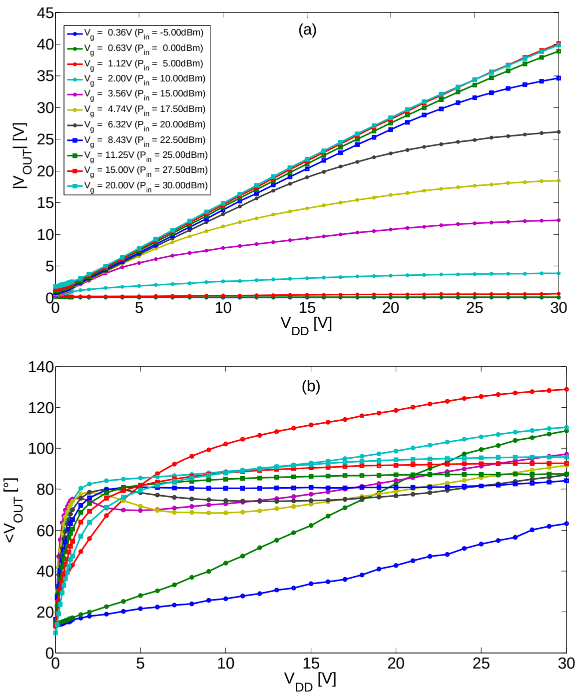


Fig. 7. a) $v_{out}(v_{DD},v_g)$ and b) $\phi_{out}(v_{DD},v_g)$ curves of the designed GaN class E PA.

The GaN class-E PA imposes very stringent requirements to be achieved by the envelope amplifier: high drain current (~1A) and a high drain voltage (30V). Moreover, as it is extendedly known, a wide bandwidth is required in the polar transmitter AM modulator. On the other hand, considering the maximum voltage provided by the digital signal generator (1V), the envelope amplifier has to provide a high voltage gain.

Taking into account all these characteristics, two cascade non-inverse amplifiers were implemented. The envelope amplifier is mainly based on a high slew-rate (900V/µs), high current (4A) and high voltage (±40V) operational amplifier from Apex Microtechnology (PA119). Therefore, the complete envelope amplifier presents a 30dB gain, 10MHz bandwidth and is capable of giving 30V and 1.2A. Unfortunately, being a continuous wave amplifier, its efficiency is not in line with the other characteristics. Nevertheless, since our goal is to study the viability of the proposed linearization technique, we incorporated it in our final test setup.

## IV. SIMULATED AND EXPERIMENTAL RESULTS

Both simulation and experimental results were obtained using a 2.5G GSM EDGE signal as input excitation (8PSK, 270.83ksym/s and 3.23dB of peak to average power ratio).

In order to evaluate the capabilities of this method, two different test sets were chosen:

(i) EER: In this case, $v_g$ is a constant envelope phase modulated RF signal and $v_{DD}$ is an amplified version of the input signal envelope;

(ii) PD: In this case both $v_g$ and $v_{DD}$ are pre-distorted signals obtained from the measured amplitude and phase characteristics of the amplifier, applying the proposed linearization technique, presented in Section II.

The first validation step was conducted using a commercial system/circuit level simulator where the two above described test sets (EER and PD) were carefully reproduced.

Fig. 8 presents the output spectra for the EER and pre-distorted cases, obtained by simulation.

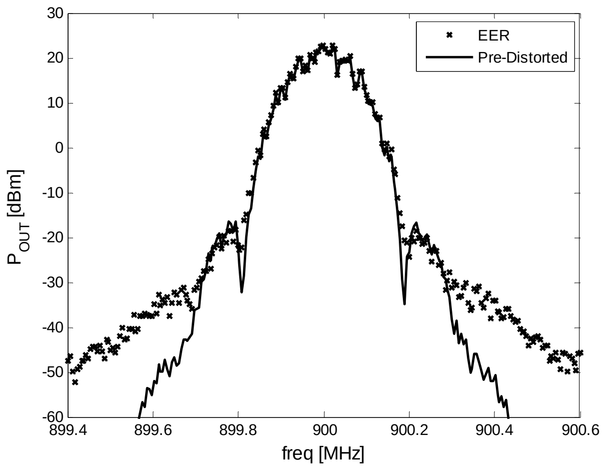


Fig. 8. Simulated output spectra for EER and PD.

As it can be observed, in the pre-distorted case, there is a significant improvement in terms of distortion, while maintaining the output power and efficiency.

These simulated results were then validated with laboratory measurements to completely prove the viability of the proposed methodology for EDGE polar transmitters.

Table I presents a performance comparison between the EER and PD cases. Results include output power (*Pout*), *PAE* and normalized mean square error (*NMSE*) figures of merit. The mean *PAE* is calculated as the statistical average, $\langle PAE(t)\rangle$, obtained from the instantaneous input, output and power supply powers delivered to the PA and the RF load. On the other hand, considering that both the input and output time domain signals are stored in two vectors with *N* samples each, the *NMSE* was estimated employing the following expression (1).

$$NMSE(dB) = 10\log_{10}\left(\frac{\sum_{n=1}^{N}\left|v_{out}(n) - k\cdot v_{in}(n)\right|^2}{\sum_{n=1}^{N}\left|k\cdot v_{in}(n)\right|^2}\right) \qquad (1)$$

This figure enables evaluating the fidelity of the obtained output signal, $v_{out}(t)$, with respect to the desired one, $k\cdot v_{in}(t)$.

Table I
Performance comparison between EER and PD

| | *Pout* | <*PAE*(*t*)> | *NMSE* |
|---|---|---|---|
| EER | 39.0dBm | 68% | -28.4dB |
| PD | 38.7dBm | 68% | -35.2dB |

In this case, the pre-distorted PA presents a normalized mean square error (*NMSE*) improvement of more than 6.5 dB, maintaining the output power (*Pout*) and average power added efficiency ($\langle PAE(t)\rangle$) figures, when they are compared with the ones obtained with the EER PA. Fig. 9 shows the measured output spectra for the EER and PD cases.

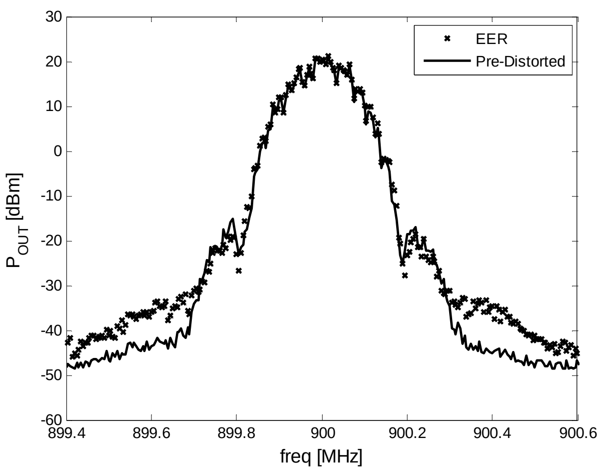


Fig. 9. Measured output spectra for EER and PD.

As it was first indicated by the results obtained with the two-tone analysis presented in [1], this linearization technique proved to be an important step towards a more linear and efficient polar transmitter, now tested with a 2.5G GSM EDGE input signal.

## V. Conclusion

In this paper, the implementation of a polar transmitter linearization procedure has been presented for a 2.5G GSM EDGE mobile communications signal. The used method complements the drain bias modulation, $v_{DD}(t)$, of conventional EER technique with a proper input drive level variation, $v_g(t)$. Good *Pout*, $\langle PAE(t)\rangle$ and *NMSE* results have been measured when the proposed pre-distortion technique has been applied to an EDGE signal.

## References


[1] P. M. Cabral, J. C. Pedro, J. A. Garcia and L. Cabria, “A Linearized Polar Transmitter for Wireless Applications”, *IEEE MTT-S Int. Microwave Symp. Dig.*, Atlanta, Georgia, USA, pp. 935-938, Jun. 2008.

[2] J. C. Pedro and N. B. Carvalho, Intermodulation Distortion in Microwave and Wireless Circuits, *Artech House*, Norwood, 2003.

[3] L. R. Kahn, “Single-Sideband transmission by envelope elimination and restoration,” *Proc. IRE*, vol. 40, no. 7, pp. 803-806, Jul. 1952.

[4] J. C. Pedro, J.A. Garcia and P. M. Cabral, “Nonlinear Distortion Analysis of Polar Transmitters”, *IEEE Trans. on Microwave Theory and Tech.*, vol. 55, issue 12, part 2, pp. 2757- 2765, Dec. 2007

[5] N. A. Sokal and A. D. Sokal, “Class-E A new class of high-efficiency tuned single-ended switching power amplifiers,” *IEEE J. Solid-State Circuits*, vol. SC-10, pp. 168-176, June 1975.

[6] T. B. Mader and Z. Popovic, “The Transmission-Line High-Efficiency Class-E Amplifiers,” *IEEE Trans. on Microwave Theory and Tech.*, vol. 43, no. 5, pp. 290-292, Sept. 1995.